

# Calcium-induced calcium release from the sarcoplasmic reticulum can be evaluated with a half-logistic function model in aequorin-injected cardiac muscles

Ju Mizuno · Kazuo Hanaoka · Mikiya Otsuji ·  
Hideko Arita · Hidetoshi Sakamoto ·  
Satoru Fukuda · Shigehito Sawamura

Received: 7 January 2011 / Accepted: 5 September 2011 / Published online: 8 October 2011  
© Japanese Society of Anesthesiologists 2011

## Abstract

**Purpose** Release of calcium ( $\text{Ca}^{2+}$ ) from the sarcoplasmic reticulum (SR) induced by  $\text{Ca}^{2+}$  influx through voltage-dependent sarcolemmal L-type  $\text{Ca}^{2+}$  channels (CICR) in cardiac muscle cells has been implicated as a potential target contributing to anesthetic-induced myocardial depression. In an earlier study, we found that (1) a half-logistic (h-L) function, which represents a half-curve of a sigmoid logistic function with a boundary at the inflection point, curve-fits the first half of the ascending phases of the isometric myocardial tension and isovolumic left ventricular (LV) pressure waveforms better than a mono-exponential (m-E) function and (2) the h-L time constants are useful as inotropic indices. We report here our investigation of the potential application of an h-L function to the analysis of the first half of the ascending phase of the  $\text{Ca}^{2+}$  transient curve (faCaT) that precedes and initiates myocardial contraction and the increase in LV pressure.

**Methods**  $\text{Ca}^{2+}$  transients (CaT) were measured using the  $\text{Ca}^{2+}$ -sensitive photoprotein aequorin, which was micro-injected into seven isolated rabbit right ventricular and 15 isolated mouse LV papillary muscles. The faCaT data from the beginning of twitch stimulation to the maximum of the first-order time derivative of  $\text{Ca}^{2+}$  concentration ( $d\text{Ca}/$

$dt_{\max}$ ) was curve-fitted by the least-squares method using h-L and m-E function equations.

**Results** The mean correlation coefficient ( $r$ ) values of the h-L and m-E curve-fits for the faCaTs were 0.9740 and 0.9654 ( $P < 0.05$ ) in the rabbit and 0.9895 and 0.9812 ( $P < 0.0001$ ) in the mouse.

**Conclusion** The h-L curves tracked the amplitudes and time courses of the faCaTs in cardiac muscles more accurately than m-E functions. Based on this result, we suggest that the h-L time constant may be a more reliable index than the m-E time constant for evaluating the rate of CICR from the SR in myocardial  $\text{Ca}^{2+}$  handling. The h-L approach may provide a more useful model for the study of CICR during the contraction process induced by anesthetic agents.

**Keywords** Myocardial contraction · Calcium transient · Curve-fit · Time constant · Calcium handling

## Introduction

Exposure to volatile anesthetic agents, such as halothane, enflurane, isoflurane, and sevoflurane, induces depression of myocardial contractility. The potent negative inotropic effects on the heart associated with volatile anesthetic agents have been well established in a variety of preparations and species. However, the molecular mechanisms underlying these effects are still not completely understood, and specific target sites explaining their relative depressant potencies have not been identified. Calcium ( $\text{Ca}^{2+}$ ) release from the sarcoplasmic reticulum (SR) induced by  $\text{Ca}^{2+}$  influx through voltage-dependent sarcolemmal L-type  $\text{Ca}^{2+}$  channels (calcium-induced calcium release; CICR) and the sensitivity of myofilaments to  $\text{Ca}^{2+}$

J. Mizuno · K. Hanaoka · M. Otsuji · H. Arita · S. Sawamura  
Department of Anesthesiology, Faculty of Medicine,  
The University of Tokyo, 7-3-1 Hongo, Bunkyo-ku,  
Tokyo 113-8655, Japan

J. Mizuno (✉) · H. Sakamoto · S. Fukuda · S. Sawamura  
Department of Anesthesiology and the Intensive Care Unit,  
Teikyo University School of Medicine, 2-11-1 Kaga,  
Itabashi-ku, Tokyo 173-8605, Japan  
e-mail: mizuno\_ju7@yahoo.co.jp

in cardiac muscle cells may be potential targets contributing to anesthetic-induced myocardial depression [1, 2]. Therefore, it would be useful to evaluate CICR from the SR in myocardial  $\text{Ca}^{2+}$  handling induced by anesthetic agents.

During each beat of the heart, a systolic rise in the intracellular  $\text{Ca}^{2+}$  concentration, referred to as a  $\text{Ca}^{2+}$  transient (CaT), precedes and initiates myocardial contraction and an increase in left ventricular (LV) pressure. Because contraction lags behind the change in intracellular  $\text{Ca}^{2+}$  concentration, the magnitude of the contraction is determined not only by the magnitude of the CaT but also by its duration. The waveforms of the CaT, myocardial tension, and LV pressure provide valuable information for evaluating intracellular  $\text{Ca}^{2+}$ , myocardial performance, and LV performance, respectively. In this paradigm, the myocardium and LV are considered to be non-linear oscillators that produce myocardial tension and LV pressure [3]. To maximize the amount of useful information extracted from the CaT, myocardial tension, and LV pressure waveforms, many investigators have attempted to curve-fit the waveforms by using various mathematical models. We previously found that the half-logistic (h-L) function, which is a half-curve of a non-linear sigmoid logistic function with a boundary at the inflection point, curve-fits the first half of the ascending phases of (1) the isometric myocardial tension curve from twitch stimulation to the maximum of the first-order time derivative of tension ( $dF/dt_{\max}$ ) [4] and (2) the isovolumic LV pressure curve from the point corresponding to QR on the electrocardiogram (ECG) to the maximum of the first-order time derivative of LV pressure ( $dP/dt_{\max}$ ) [5] better than the mono-exponential (m-E) function. The first half of the ascending phase of the CaT curve (faCaT) is expected to change in parallel with the amplitudes and time courses of the myocardial tension and LV pressure curves. We speculated that the faCaT could also be represented as an h-L function curve.

In the study reported here, we investigated the potential application of the h-L function to the analysis of the faCaT in cardiac muscles and sought to determine whether h-L functions curve-fit more accurately than m-E functions. Improved curve-fit by using the best-fit h-L function would provide a superior time constant and add to our understanding of CICR from the SR in myocardial  $\text{Ca}^{2+}$  handling and excitation–contraction (E–C) coupling during the contraction process induced by anesthetic agents.

## Methods

This study protocol was approved by the Animal Investigation Committee of the Jikei University School of Medicine. All procedures during the experiments were

conducted in the Jikei University School of Medicine in conformity with the “Guiding principles for the care and use of animals in the field of physiological sciences” endorsed by the American Physiological Society and the Physiological Society of Japan.

## Surgical preparation

The experimental procedures have been previously described in detail [4, 6, 7]. In short, seven albino rabbits (Japan White; body weight 2.0–2.5 kg) and 15 mice (C57BL/6; body weight 25–30 g) were anesthetized with intravenous (1.5–2.0 mg/kg) and intraperitoneal (15–20 mg/kg) pentobarbital sodium, respectively. Following removal of the heart, the aorta was cannulated with a blunted 18 G needle, and the heart was mounted on a Langendorff apparatus. The coronary blood was washed out with Tyrode’s solution containing 2 mM  $\text{Ca}^{2+}$  buffered by *N*-2-hydroxyethyl-piperazine-*N*-2-ethanesulfonic acid (HEPES) at a constant pressure for 5 min. The solution was changed to HEPES-buffered Tyrode’s solution containing 2 mM  $\text{Ca}^{2+}$  and 20 mM 2, 3-butanedione monoxime (BDM) after the heart beat was stabilized. Once the contraction stopped completely, the heart was removed from the Langendorff apparatus. A thin papillary muscle was dissected out from the rabbit right ventricular (RV) and mouse LV walls.

After both ends of the isolated muscle had been tied with silk threads, the muscle was mounted horizontally in an experimental chamber, immersed in a bath, and continuously perfused with Tyrode’s solution. One end of the muscle was attached to a fixed hook, and the other was attached to the arm of a tension transducer (BG-10; Kulite Semiconductor Products, Leonia, NJ; compliance 2.5  $\mu\text{m/g}$ , unloaded resonant frequency 0.6 kHz). A pair of platinum black electrodes was placed parallel to the muscle, which was regularly stimulated by a single square pulse of 5 ms duration and 0.2 Hz; the strength of the stimulation was 1.5-fold the threshold. The muscle was slowly stretched and adjusted to the length at which the developed tension reached maximum ( $L_{\max}$ ).

## Aequorin injection

Aequorin was dissolved in 150 mM KCl and 5 mM HEPES, pH 7.0, at a final concentration of 50–100  $\mu\text{M}$ . Using glass micropipettes with a resistance of 30–50 M $\Omega$ , we injected aequorin into 150–200 superficial cells of the preparation using nitrogen gas. Aequorin light signals were detected using a photomultiplier (EMI 9789A; Thorn EMI, Ruislip, UK) placed just above the muscle [8]. In twitch response, the aequorin light signal was recorded through a 500-Hz low-pass filter. Aequorin light signals were

converted to cytoplasmic  $Ca^{2+}$  concentration units using an in vitro calibration curve [9–11]. Sixty-four aequorin light signals were averaged to improve the signal-to-noise ratio.  $Ca^{2+}$  signals were sampled at 1-ms intervals and digitized with an A/D converter. All  $Ca^{2+}$  data were stored on tape (NFR-3515W; Sony-Magnescape, Tokyo, Japan) and a computer (PC-9801; NEC, Tokyo, Japan) for later analysis.

**Tyrode’s solution**

Tyrode’s solution buffered with HEPES was used during all experiments, including muscle dissection and aequorin injection. The composition of the solution (in mM) was as follows: NaCl, 136.9; KCl, 5.4;  $MgCl_2$ , 0.5;  $NaH_2PO_4$ , 0.33; HEPES, 5; glucose, 5. The pH was adjusted to  $7.40 \pm 0.05$  with NaOH at 24°C, and the solution was equilibrated with 100%  $O_2$ . The temperature of the solution was continuously monitored with a thermocouple and maintained at  $30 \pm 0.5^\circ C$ .

**$Ca^{2+}$  transients**

$Ca^{2+}$  signals were measured from the point before the twitch stimulation procedure was started. The  $Ca^{2+}$  signal gradually increased, reached a peak, then decreased and returned to the resting  $Ca^{2+}$  concentration before the following twitch stimulation—all within the 1,000-ms sampling window. Signals for the faCaT, which extends from the point that twitch stimulation begins to the point corresponding to the maximum of the first-order time derivative of  $Ca^{2+}$  concentration ( $dCa/dt_{max}$ ), were used for subsequent analyses. The  $dCa/dt$  was obtained by differentiating the sampled  $Ca^{2+}$  data after digital smoothening using an 11-point, non-weighted moving average of digitized  $Ca^{2+}$  data signals.

**h-L function equation**

The following h-L function was used to curve-fit the faCaT data by the least-squares method in DeltaGraph ver. 4.0 (DeltaPoint, Monterey, CA) as shown in Fig. 1a:

$$Ca(t) = 2Ca_A / \{1 + \exp[-(t - t_C) / Ca\tau_L]\} + Ca_B \quad (1)$$

where  $t$  is the time from the beginning of twitch stimulation to the point corresponding to  $dCa/dt_{max}$ ,  $Ca_A$  is the h-L amplitude constant,  $Ca\tau_L$  is the h-L time constant,  $Ca_B$  is the h-L non-zero asymptote, and  $t_C$  is a constant. The h-L function curve given by Eq. 1 increases monotonically from  $Ca(0) (=Ca_B)$  to  $Ca(Ca\tau_C) [(Ca_A + Ca_B)]$ . The  $Ca\tau_L$  value corresponds to the time for the curves to increase from  $Ca(t_C - Ca\tau_L) \{=[2Ca_A / (1 + e) + Ca_B]\}$  to  $Ca(t_C) [(Ca_A + Ca_B)]$ .  $Ca(t_C - Ca\tau_L)$  is  $2 / (1 + e)$  ( $\sim 0.54$ ) of  $Ca_A$  plus  $Ca_B$ . The  $t_C$  value represents the time at  $dCa/dt_{max}$ .

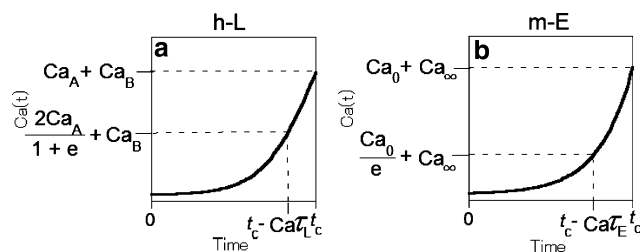


**Fig. 1** Half-logistic (*h-L*) and mono-exponential (*m-E*) distribution function curves for the first half of the ascending phase of the  $Ca^{2+}$  transient curve (faCaT). **a** The *h-L* function curve described by Eq. 1.  $Ca_A$  *h-L* amplitude constant,  $Ca\tau_L$  *h-L* time constant,  $Ca_B$  *h-L* non-zero asymptote,  $t_C$  time at the maximum of the first-order time derivative of  $Ca^{2+}$  concentration ( $dCa/dt_{max}$ ). **b** The *m-E* function curve described by Eq. 2.  $Ca_0$  *m-E* amplitude constant,  $Ca\tau_E$  *m-E* time constant,  $Ca_\infty$  *m-E* non-zero asymptote,  $t_C$  time at  $dCa/dt_{max}$

**m-E function equation**

An *m-E* function was also used to curve-fit the faCaT data by the least-squares method, as shown in Fig. 1b:

$$Ca(t) = Ca_0 \exp[(t - t_C) / Ca\tau_E] + Ca_\infty \quad (2)$$

where  $t$  is the time from the point that twitch stimulation begins,  $Ca_0$  is the *m-E* amplitude constant,  $Ca\tau_E$  is the *m-E* time constant,  $Ca_\infty$  is the *m-E* non-zero asymptote, and  $t_C$  is a constant. The *m-E* function curve given by Eq. 2 increases monotonically from  $Ca(0) (=Ca_\infty)$  to  $Ca(t_C) [(Ca_0 + Ca_\infty)]$ . The  $Ca\tau_E$  value corresponds to the time for the curve to increase from  $Ca(t_C - Ca\tau_E) [(Ca_0 / e + Ca_\infty)]$  to  $Ca(t_C) [(Ca_0 + Ca_\infty)]$ .  $Ca(t_C - Ca\tau_E)$  is  $1/e$  ( $\sim 0.37$ ) of  $Ca_0$  plus  $Ca_\infty$ . The  $t_C$  value represents the time at  $dCa/dt_{max}$ .

It should be noted that *h-L* function (Eq. 1) has the same number of parameters—three—as the *m-E* function (Eq. 2) and that  $Ca_A$ ,  $Ca\tau_L$ , and  $Ca_B$  in Eq. 1 are conceptually similar to  $Ca_0$ ,  $Ca\tau_E$ , and  $Ca_\infty$  in Eq. 2, respectively.

**Statistical analysis**

Goodness of fit was evaluated with the correlation coefficient ( $r$ ) and residual mean squares (RMS) for the *h-L* and *m-E* curve-fitting models. Fisher’s  $Z$  transformation ( $Z$ ) of  $r$  [12] was calculated with the following equation:  $Z = 1/2[\ln(1 + r) - \ln(1 - r)]$ . Residual values were calculated as the observed faCaT data minus the best-fit *h-L* or *m-E* value at each sampling data point. RMS was calculated as the residual sum of squares divided by the residual degrees of freedom, which indicates the number of data points analyzed minus the number of parameters in the function [13].

The  $Z$  of  $r$  and RMS values were compared between the goodness of *h-L* and *m-E* fits by a paired Student’s  $t$  test. The *h-L* and *m-E*  $Z$  of  $r$ , RMS,  $Ca_A$ ,  $Ca\tau_L$ ,  $Ca_B$ ,  $Ca_0$ ,  $Ca\tau_E$ ,

and  $Ca_{\infty}$  values between rabbit and mouse were compared by an unpaired Student's *t* test.

Analyses were performed using Statcel (OMS, Saitama, Japan) and StatView ver. 5.0 (SAS Institute, Cary, NC) software. Values in the text are expressed as the mean  $\pm$  standard deviation (SD) unless otherwise noted. A *P* value of  $<0.05$  was considered to indicate statistical significance.

**Results**

Measurements of rising phases of CaT

The mean diameters of the isolated muscle specimens in the seven rabbits and 15 mice were  $0.73 \pm 0.13$  and  $0.63 \pm 0.11$  mm, respectively. The mean muscle lengths of each rabbit and mouse were  $3.30 \pm 0.77$  and  $2.01 \pm 0.43$  mm, respectively.

Table 1 summarizes the representative values observed from the entire time course of CaT data. The  $Ca^{2+}$  concentration at  $dCa/dt_{max}$  and peak  $Ca^{2+}$  concentration in the rabbit were significantly lower than those in the mouse. The time to  $dCa/dt_{max}$  and time to peak  $Ca^{2+}$  concentration in the rabbit were significantly longer than those in the mouse. The  $dCa/dt_{max}$  in the rabbit was significantly less positive than that in the mouse.

h-L and m-E curve-fits

The representative best-fitted h-L and m-E function curves for the observed faCaT data in a rabbit muscle and mouse muscle are shown in Fig. 2a, b and Fig. 3a, b, respectively.

**Table 1** Observed values of  $Ca^{2+}$  transients

| Observed value                                     | Rabbit                | Mouse            |
|--|-----------------------|------------------|
| $Ca^{2+}$ concentration at $dCa/dt_{max}$ (nmol/l) | $295 \pm 94^{**}$     | $819 \pm 189$    |
| Peak $Ca^{2+}$ concentration (nmol/l)              | $718 \pm 96^{**}$     | $1694 \pm 384$   |
| Time to $dCa/dt_{max}$ (ms)                        | $64.7 \pm 2.8^{**}$   | $60.1 \pm 1.4$   |
| Time to peak $Ca^{2+}$ concentration (ms)          | $105.4 \pm 24.2^{**}$ | $76.1 \pm 2.1$   |
| $dCa/dt_{max}$ (nmol/l/ms)                         | $41.4 \pm 12.6^{**}$  | $119.8 \pm 28.7$ |

Data are presented as the mean  $\pm$  standard deviation (SD) of the observed values of the  $Ca^{2+}$  transient (CaT) curves in papillary muscles dissected from the right ventricular (RV) walls of seven rabbits and left ventricular (LV) walls of 15 mice

$dCa/dt_{max}$ , Maximum of the first-order time derivative of  $Ca^{2+}$  concentration

\*\* *P* < 0.0001 versus mouse

Goodness of h-L and m-E fits

The goodness of h-L and m-E fits for the faCaT data are listed in Table 2. The h-L *Z* values were significantly higher than the m-E *Z* values in both the rabbit and mouse, while the h-L RMS values were significantly lower than the m-E RMS values in both the rabbit and mouse.

Best-fitted h-L and m-E parameters

Table 3 summarizes the calculated h-L and m-E function parameters for the faCaTs. The  $Ca_A$  and  $Ca_0$  values in the rabbit were significantly smaller than those in the mouse. The  $Ca\tau_L$  and  $Ca\tau_E$  values and the  $Ca_B$  and  $Ca_{\infty}$  values in the rabbit were not significantly different from those in the mouse.

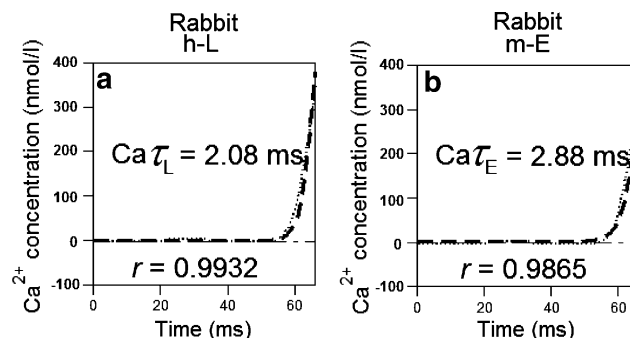


**Fig. 2** Representative best-fitted h-L and m-E function curves for faCaT in rabbit. **a, b** Representative best-fitted h-L and m-E function curves (thick broken lines) for the faCaT from the point of the beginning of twitch stimulation to the point corresponding to  $dCa/dt_{max}$  (thin dotted line) in a rabbit right ventricular papillary muscle. *r* Correlation coefficient; see caption to Fig. 1 for other abbreviations

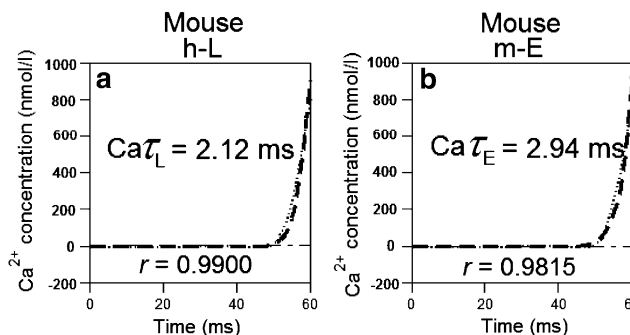


**Fig. 3** Representative best-fitted h-L and m-E function curves for faCaT in mouse. **a, b** Representative best-fitted h-L and m-E function curves (thick broken lines) for the faCaT from the point of the beginning of twitch stimulation to the point corresponding to  $dCa/dt_{max}$  (thin dotted line) in a mouse left ventricular papillary muscle. See captions to Figs. 1 and 2 for abbreviations

**Table 2** Goodness of half-logistic and mono-exponential distribution function curve fits for the first half of the ascending phase of the Ca<sup>2+</sup> transient curve

| Goodness of fit <sup>a</sup> | Rabbit        |             | Mouse         |             |
|------------------------------|---------------|-------------|---------------|-------------|
|                              | h-L           | m-E         | h-L           | m-E         |
| <i>r</i>                     | 0.9740        | 0.9654      | 0.9895        | 0.9812      |
| <i>Z</i>                     | 2.16 ± 0.44** | 2.02 ± 0.37 | 2.62 ± 0.19** | 2.33 ± 0.14 |
| RMS (nmol/l) <sup>2</sup>    | 268 ± 300*    | 327 ± 343   | 627 ± 320*    | 1090 ± 519  |

*h-L*, *m-E*, Half-logistic and mono-exponential distribution function curves, respectively

\* *P* < 0.05, \*\* *P* < 0.0001 versus m-E

<sup>a</sup> The correlation coefficient (*r*) value indicates the mean after *Z* transformation (*Z*); *Z* and residual mean squares (RMS) values indicate the mean ± SD of h-L and m-E curve-fits for the first half of the ascending CaT curves (faCaT) from the point of the beginning of twitch stimulation to the point corresponding to dCa/dt<sub>max</sub> in papillary muscles dissected from the RV walls of seven rabbits and LV walls of 15 mice

**Table 3** Calculated h-L and m-E distribution function parameters of curve-fits for faCaT

| Calculated value         | Rabbit      | Mouse       |
|--------------------------|-------------|-------------|
| Ca <sub>A</sub> (nmol/l) | 310 ± 101** | 869 ± 199   |
| Ca <sub>0</sub> (nmol/l) | 320 ± 104** | 899 ± 206   |
| Caτ <sub>L</sub> (ms)    | 2.29 ± 0.30 | 2.22 ± 0.16 |
| Caτ <sub>E</sub> (ms)    | 3.18 ± 0.43 | 3.08 ± 0.23 |
| Ca <sub>B</sub> (nmol/l) | 5.5 ± 6.1   | 1.5 ± 5.8   |
| Ca <sub>∞</sub> (nmol/l) | 4.9 ± 6.1   | −0.2 ± 5.9  |

Data are presented as the mean ± SD of calculated h-L and m-E function parameters of curve-fits for the faCaT from the point of the beginning of twitch stimulation to the point corresponding to dCa/dt<sub>max</sub> in papillary muscles dissected from the RV walls of seven rabbits and LV walls of 15 mice

Ca<sub>A</sub>, h-L amplitude constant; Ca<sub>0</sub>, m-E amplitude constant; Caτ<sub>L</sub>, h-L time constant; Caτ<sub>E</sub>, m-E time constant; Ca<sub>B</sub>, h-L non-zero asymptote; Ca<sub>∞</sub>, m-E non-zero asymptote

\*\* *P* < 0.0001 versus mouse

**Discussion**

The results of our experiments demonstrate that h-L functions curve-fit the faCaTs more accurately than m-E functions in both rabbit and mouse papillary muscles. Therefore, we suggest that an h-L function model could be used to characterize more reliably the amplitude and time course of the faCaT in cardiac muscles.

**h-L function model**

Curve-fitting and non-linear regression may be valuable tools for elucidating mechanisms, summarizing information, removing noise, allowing speculation regarding unmeasured data, and separating out the effects of multiple factors.

The logistic function has been widely used to study rising phenomena in many fields of bioscience and to describe intuitively symmetrical sigmoid curves whose

inflection point corresponds to the boundary, such as those found in mortality data [14] and growth curves [15, 16]. The logistic nature of these phenomena predicts that the process is initially minimal, gradually increases, and maximizes to an asymptote. The logistic function is limited in its ability to represent the sigmoid function, especially as it reaches the upper asymptote. In a previous study, we reported that the logistic function curve-fits well the ascending phase from twitch stimulation to the peak Ca<sup>2+</sup> concentration [7]. A computer simulation of the CaT also provided a characterization of the logistic function [17]. The inflection point of the ascending phase of the CaT is dCa/dt<sub>max</sub>, which corresponds to the end point of the faCaT.

The logistic function is used as the solution to the differential equation  $dN/dt = kN(N_0 - N)$ . As a simple model of intracellular Ca<sup>2+</sup> handling, we hypothesize that all intracellular Ca<sup>2+</sup> concentrations are derived from the SR. Because the SR is the major source of Ca<sup>2+</sup> for contraction, most Ca<sup>2+</sup> flows into the cytoplasm by CICR, with only a small amount of Ca<sup>2+</sup> flowing into the cytoplasm via L-type Ca<sup>2+</sup> channels. We hypothesize that the SR has *N*<sub>0</sub> Ca<sup>2+</sup> in the stable situation. If *N* of Ca<sup>2+</sup> is released from the SR by CICR, the cytoplasm includes *N* of Ca<sup>2+</sup>, and the SR includes (*N*<sub>0</sub> − *N*) of Ca<sup>2+</sup>. If the rate of Ca<sup>2+</sup> release from the SR is dependent on the remaining Ca<sup>2+</sup> in the SR, the amount of Ca<sup>2+</sup> per time is *k*(*N*<sub>0</sub> − *N*). The greater the inflow of Ca<sup>2+</sup> into the cytoplasm via L-type Ca<sup>2+</sup> channels, the more Ca<sup>2+</sup> is released from the SR by CICR. Therefore, the amount of Ca<sup>2+</sup> released per time is *kN*(*N*<sub>0</sub> − *N*). From this model, Ca<sup>2+</sup> released from the SR by CICR could be curve-fitted by the logistic function. The transient increase in cytoplasmic Ca<sup>2+</sup> concentration induces a transient increase in the binding of Ca<sup>2+</sup> to a major Ca<sup>2+</sup>-binding protein, troponin C (TnC), a transient increase in attachment of the thick filament myosin cross-bridge (CB) to thin filament actin, and myocardial contraction. Curve-fitting for the faCaT by the h-L function

would be useful for evaluating the time constant of CICR and the effect of cytoplasmic  $\text{Ca}^{2+}$  on CICR from the SR.

In comparison, the m-E function is used to model phenomena when a constant change in the independent variable gives the same proportional change. Then, the graph of the m-E function indicates when a quantity increases at a rate proportional to its current value.

The faCaT is predictable from the best-fitted h-L function curve.  $\text{Ca}\tau_L$  for the faCaT may be a more reliable index of the rate of increase in myocardial intracellular  $\text{Ca}^{2+}$  concentration than  $\text{Ca}\tau_E$ . The  $\text{Ca}^{2+}$  concentration calculated from the h-L function may produce more reliable values than the values of the CaT observed by sampling at the rate of 1 kHz. Thus, it may be possible to obtain significant insight into CICR in myocardial  $\text{Ca}^{2+}$  handling and E-C coupling during the contraction process by analysis using the h-L function.

The rate of increase in  $\text{Ca}^{2+}$  concentration gradually increases from twitch stimulation, ultimately reaching a maximum at  $d\text{Ca}/dt_{\text{max}}$ . We speculate that  $d\text{Ca}/dt_{\text{max}}$  corresponds to the maximum rate of  $\text{Ca}^{2+}$  concentration released by CICR. In clinical practice, the  $dF/dt_{\text{max}}$  and  $dP/dt_{\text{max}}$  values are commonly used as indices of myocardial and LV inotropism. We observed the  $d\text{Ca}/dt_{\text{max}}$  value by measuring the CaT every 1 ms. However, the CaT data include noise, which could affect the measurement of  $d\text{Ca}/dt$ . We therefore obtained a more reliable  $d\text{Ca}/dt_{\text{max}}$  value by curve-fitting with the h-L function.

The calculated h-L function parameters were able to summarize the amplitude and time course of the faCaT, with almost no loss of information on the characteristics of the curve. The calculated  $\text{Ca}_A$ ,  $\text{Ca}\tau_L$ , and  $\text{Ca}_B$  may have physiological as well as mathematical meanings. The h-L amplitude constant  $\text{Ca}_A$  represents the  $\text{Ca}^{2+}$  concentration at the maximum rate of  $\text{Ca}^{2+}$  concentration released by CICR from the SR in myocardial  $\text{Ca}^{2+}$  handling. The h-L time constant  $\text{Ca}\tau_L$  represents the time from  $2/(1 + e)$  of  $\text{Ca}_A$  plus  $\text{Ca}_B$  to  $\text{Ca}_A$  plus  $\text{Ca}_B$  and evaluates the rate of CICR. The h-L non-zero asymptote  $\text{Ca}_B$  represents the resting myocardial intracellular  $\text{Ca}^{2+}$  concentration before twitch stimulation (Fig. 1). We were able to compare the amplitudes and time courses of the faCaTs using the calculated h-L function parameters.

#### Anesthetic agents

The potent negative inotropic effect on the heart depends on the anesthetic agent. Halothane has greater depressant contractile force effects on the canine cardiac Purkinje fibers than isoflurane at an equivalent minimum alveolar concentration [18]. Halothane also depresses cardiac systolic function more than sevoflurane and isoflurane in

the isolated perfused rat heart [19]. These findings demonstrate that the alteration in intracellular  $\text{Ca}^{2+}$  concentration during the contraction process is differentially altered by anesthetic agents. Halothane decreases contractile force and intracellular CaT more than isoflurane in guinea pig RV papillary muscle [20]. Enflurane causes a greater depression of the caffeine-induced intracellular  $\text{Ca}^{2+}$  concentration than isoflurane in rat ventricular myocytes [21]. These effects may result from stimulation of the CICR mechanism, which depletes the SR of  $\text{Ca}^{2+}$  stores. Halothane and enflurane, but not isoflurane, increase the binding of radiolabeled ryanodine to the porcine SR [22]. The h-L approach allows direct comparison of the negative inotropic effects of volatile anesthetic agents on contractile properties and myocardial  $\text{Ca}^{2+}$  handling, and provides further insight into the mechanisms contributing to their depressant action on the heart.

#### Species differences

The molecular details of myocardial  $\text{Ca}^{2+}$  handling depend on the species [23]. Species differences are mainly dependent on CICR [24], SR  $\text{Ca}^{2+}$ -ATPase activity [25], and  $\text{Na}^+$ - $\text{Ca}^{2+}$  exchange [26]. For instance, exposure to increasing concentrations of ryanodine diminishes the contractile ability of rat cardiac muscle dramatically; dog and cat cardiac muscles show intermediate effects, while the contractile performance of the rabbit preparation is relatively little affected [27]. The rise in intracellular  $\text{Ca}^{2+}$  in rat myocytes is markedly dependent on ryanodine-sensitive release of  $\text{Ca}^{2+}$  from the SR compared with guinea pig myocytes [28]. The contraction that develops in rat myocytes is fully inhibited by 0.1  $\mu\text{M}$  ryanodine, but the contraction of guinea pig myocytes is only slightly reduced by 1  $\mu\text{M}$  ryanodine. In addition, rat myocytes are rather insensitive to the  $\text{Ca}^{2+}$  blocker nifedipine, while the contraction of guinea pig myocytes is greatly suppressed by this  $\text{Ca}^{2+}$  blocker [29]. The CICR mechanism of the SR in the rat heart is more developed than that in the rabbit heart [30]. In mouse myocytes, the peak L-type  $\text{Ca}^{2+}$  current is smaller, but the SR  $\text{Ca}^{2+}$  content, SR  $\text{Ca}^{2+}$ -ATPase activity, and outward  $\text{Na}^+$ - $\text{Ca}^{2+}$  exchange current are greater than those in rabbit myocytes [24, 25].

Our results show that the  $\text{Ca}^{2+}$  concentrations at  $d\text{Ca}/dt_{\text{max}}$ ,  $\text{Ca}_A$ , and  $\text{Ca}_0$  in the mouse are higher than those in the rabbit, although the time to  $d\text{Ca}/dt_{\text{max}}$  and the time to peak  $\text{Ca}^{2+}$  concentration in the mouse are shorter than those in the rabbit (Tables 1, 3). Moreover,  $d\text{Ca}/dt_{\text{max}}$  in the mouse is more positive than that in the rabbit, but  $\text{Ca}\tau_L$  and  $\text{Ca}\tau_E$  in the mouse are similar to those in the rabbit. These findings may be consistent with substantial species differences.

## Limitations

There are a number of limitations to this study. First, it was limited to a study of two animal species. An investigation in other species is needed to understand species differences more fully. Second, the muscle lengths of rabbit RV and mouse LV were suitable for the experimental chamber. Alternate LV or RV papillary muscles should be used to assess species differences. Furthermore, CaTs should be compared in single cardiac cells. Third, the experimental condition used to measure the faCaT was not physiological, i.e., 100%  $L_{\max}$  with 2 mM extracellular  $\text{Ca}^{2+}$  at 30°C and a stimulation frequency of 0.2 Hz. Further examination of these concepts is needed under physiological conditions, such as different preloads,  $\text{Ca}^{2+}$  concentrations, temperatures, and pharmacological conditions with block or stimulation of channels, pumps, exchangers, and anesthetic agents. Fourth, we used the  $\text{Ca}^{2+}$ -sensitive photoprotein aequorin, which is a good indicator of change in intracellular  $\text{Ca}^{2+}$  concentration. Additional investigations with other  $\text{Ca}^{2+}$ -sensitive indicators, such as Indo 1 and Fura 2, would be useful. Finally, we curve-fitted the faCaT using the h-L and m-E function models with three parameters, i.e., amplitude constants, time constants, and non-zero asymptotes. We intend to develop the h-L function with an additional parameter or a new function to curve-fit it more accurately.

## Conclusion

Based on these results, we conclude that h-L functions are able to describe the amplitudes and time courses of the faCaTs more accurately than m-E functions in both rabbit RV and mouse LV papillary muscles.  $\text{Ca}\tau_L$  may be a more reliable index to evaluate the rate of CICR from the SR in myocardial  $\text{Ca}^{2+}$  handling than  $\text{Ca}\tau_E$ . The h-L approach may provide a more useful model for studying CICR during the contraction process induced by anesthetic agents.

**Acknowledgments** We would like to thank Drs. Shuta Hirano, Yoichiro Kusakari, and Satoshi Kurihara at the Department of Cell Physiology, The Jikei University School of Medicine, for their excellent research assistance.

## References

1. Wilde DW, Knight PR, Sheth N, Williams BA. Halothane alters control of intracellular  $\text{Ca}^{2+}$  mobilization in single rat ventricular myocytes. *Anesthesiology*. 1991;75:1075–86.
2. Connelly TJ, Coronado R. Activation of the  $\text{Ca}^{2+}$  release channel of cardiac sarcoplasmic reticulum by volatile anesthetics. *Anesthesiology*. 1994;81:459–69.
3. Eucker SA, Lissauskas JB, Singh J, Kovács SJ. Phase plane analysis of left ventricular hemodynamics. *J Appl Physiol*. 2001;90:2238–44.
4. Mizuno J, Morita S, Otsuji M, Arita H, Hanaoka K, Akins RE, Hirano S, Kusakari Y, Kurihara S. Half-logistic time constants as inotropic and lusitropic indices for four sequential phases of isometric tension curve in isolated rabbit and mouse papillary muscles. *Int Heart J*. 2009;50:389–404.
5. Mizuno J, Shimizu J, Mohri S, Araki J, Hanaoka K, Yamada Y. Hypovolemia does not affect speed of isovolumic left ventricular contraction and relaxation in excised canine heart. *Shock*. 2008;29:395–401.
6. Mizuno J, Otsuji M, Takeda K, Yamada Y, Arita H, Hanaoka K, Hirano S, Kusakari Y, Kurihara S. Superior logistic model for decay of  $\text{Ca}^{2+}$  transient and isometric relaxation force curve in rabbit and mouse papillary muscles. *Int Heart J*. 2007;48:215–32.
7. Mizuno J, Otsuji M, Arita H, Hanaoka K, Morita S, Akins R, Hirano S, Kusakari Y, Kurihara S. Characterization of intracellular  $\text{Ca}^{2+}$  transient by the hybrid logistic function in aequorin-injected rabbit and mouse papillary muscles. *J Physiol Sci*. 2007;57:349–59.
8. Allen DG, Kurihara S. The effects of muscle length on intracellular calcium transients in mammalian cardiac muscle. *J Physiol*. 1982;327:79–94.
9. Allen DG, Blinks JR, Prendergast FG. Aequorin luminescence: relation of light emission to calcium concentration—a calcium-independent component. *Science*. 1977;195:996–8.
10. Blinks JR, Wier WG, Hess P, Prendergast FG. Measurement of  $\text{Ca}^{2+}$  concentrations in living cells. *Prog Biophys Mol Biol*. 1982;40:1–114.
11. Okazaki O, Suda N, Hongo K, Konishi M, Kurihara S. Modulation of  $\text{Ca}^{2+}$  transients and contractile properties by beta-adrenoceptor stimulation in ferret ventricular muscles. *J Physiol*. 1990;423:221–40.
12. Snedecor GW, Cochran WG. *Statistical methods*. 6th edn. Ames: Iowa State University Press; 1971. p. 185.
13. Thompson DS, Waldron CB, Coltart DJ, Jenkins BS, Webb-Peplee MM. Estimation of time constant of left ventricular relaxation. *Br Heart J*. 1983;49:250–8.
14. Wilson DL. The analysis of survival (mortality) data: fitting Gompertz, Weibull, and logistic functions. *Mech Ageing Dev*. 1994;74:15–33.
15. Sheehy JE, Mitchell PL, Ferrer AB. Bi-phasic growth patterns in rice. *Ann Bot (Lond)*. 2004;94:811–7.
16. Fujikawa H, Morozumi S. Modeling surface growth of *Escherichia coli* on agar plates. *Appl Environ Microbiol*. 2005;71:7920–6.
17. Sakamoto T, Matsubara H, Hata Y, Shimizu J, Araki J, Takaki M, Suga H. Logistic character of myocardial twitch force curve: simulation. *Heart Vessels*. 1996;11:171–9.
18. Stowe DF, Sprung J, Turner LA, Kampine JP, Bosnjak ZJ. Differential effects of halothane and isoflurane on contractile force and calcium transients in cardiac Purkinje fibers. *Anesthesiology*. 1994;80:1360–8.
19. Skeehean TM, Schuler HG, Riley JL. Comparison of the alteration of cardiac function by sevoflurane, isoflurane, and halothane in the isolated working rat heart. *J Cardiothorac Vasc Anesth*. 1995;9:706–12.
20. Bosnjak ZJ, Aggarwal A, Turner LA, Kampine JM, Kampine JP. Differential effects of halothane, enflurane, and isoflurane on  $\text{Ca}^{2+}$  transients and papillary muscle tension in guinea pigs. *Anesthesiology*. 1992;76(1):123–31.
21. Wilde DW, Davidson BA, Smith MD, Knight PR. Effects of isoflurane and enflurane on intracellular  $\text{Ca}^{2+}$  mobilization in isolated cardiac myocytes. *Anesthesiology*. 1993;79:73–82.

22. Connelly TJ, Hayek RE, Rusy BF, Coronado R. Volatile anesthetics selectively alter [<sup>3</sup>H]ryanodine binding to skeletal and cardiac ryanodine receptors. *Biochem Biophys Res Commun.* 1992;186:595–600.
23. Bassani JWM, Bassani RA, Bers DM. Relaxation in rabbit and rat cardiac cells: species-dependent differences in cellular mechanisms. *J Physiol.* 1994;476:279–93.
24. Su Z, Sugishita K, Li F, Ritter M, Barry WH. Effects of FK506 on [Ca<sup>2+</sup>]<sub>i</sub> differ in mouse and rabbit ventricular myocytes. *J Pharmacol Exp Ther.* 2003;304:334–41.
25. Su Z, Li F, Spitzer KW, Yao A, Ritter M, Barry WH. Comparison of sarcoplasmic reticulum Ca<sup>2+</sup>-ATPase function in human, dog, rabbit, and mouse ventricular myocytes. *J Mol Cell Cardiol.* 2003;35:761–7.
26. Su Z, Bridge JH, Philipson KD, Spitzer KW, Barry WH. Quantitation of Na/Ca exchanger function in single ventricular myocytes. *J Mol Cell Cardiol.* 1999;31:1125–35.
27. Sutko JL, Willerson JT. Ryanodine alteration of the contractile state of rat ventricular myocardium. Comparison with dog, cat, and rabbit ventricular tissues. *Circ Res.* 1980;46:332–43.
28. Mitchell MR, Powell T, Terrar DA, Twist VW. Calcium-activated inward current and contraction in rat and guinea-pig ventricular myocytes. *J Physiol.* 1987;391:545–60.
29. Horackova M. Possible role of Na<sup>+</sup>-Ca<sup>2+</sup> exchange in the regulation of contractility in isolated adult ventricular myocytes from rat and guinea pig. *Can J Physiol Pharmacol.* 1989;67:1525–33.
30. Fabiato A. Calcium release in skinned cardiac cells: variations with species, tissues, and development. *Fed Proc.* 1982;41:2238–44.